

Supplementary Figure S1

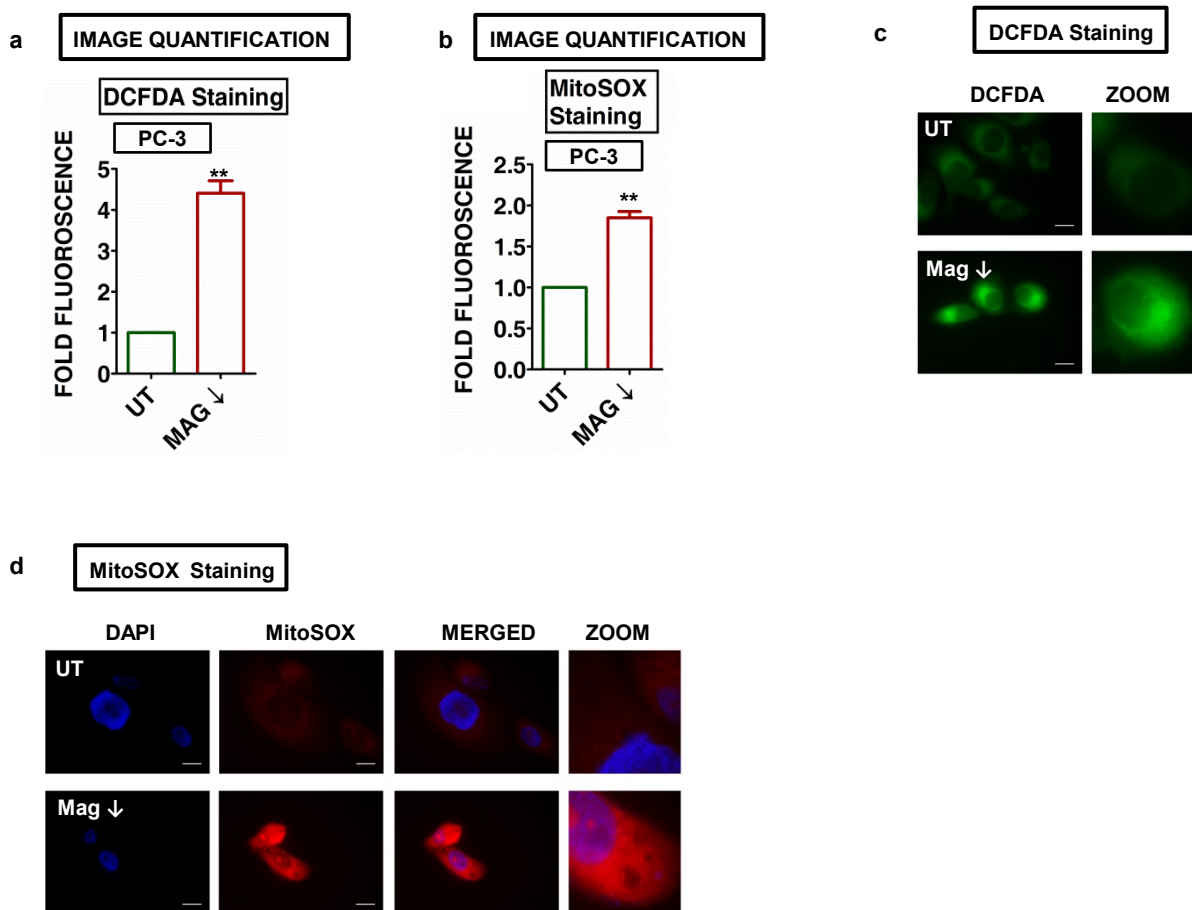


Figure S1 (a, b) Quantification of fluorescence in microscopic images of PC-3 cells (shown in Figure 1h-i) stained with DCFDA (a) and MitoSOX (b) using ImageJ software. Uniform area of the fields shown in respective panel corresponding to single cell was selected and quantified for the change in fluorescent intensity of respective dyes. Data represented as mean \pm SEM, $n=3$, $**P<0.05$ (two tailed). (c, d) Microscopic images of PC-3 cells with lower expression of Magmas and stained with DCFDA (c) and MitoSOX (d).

Supplementary Figure S2

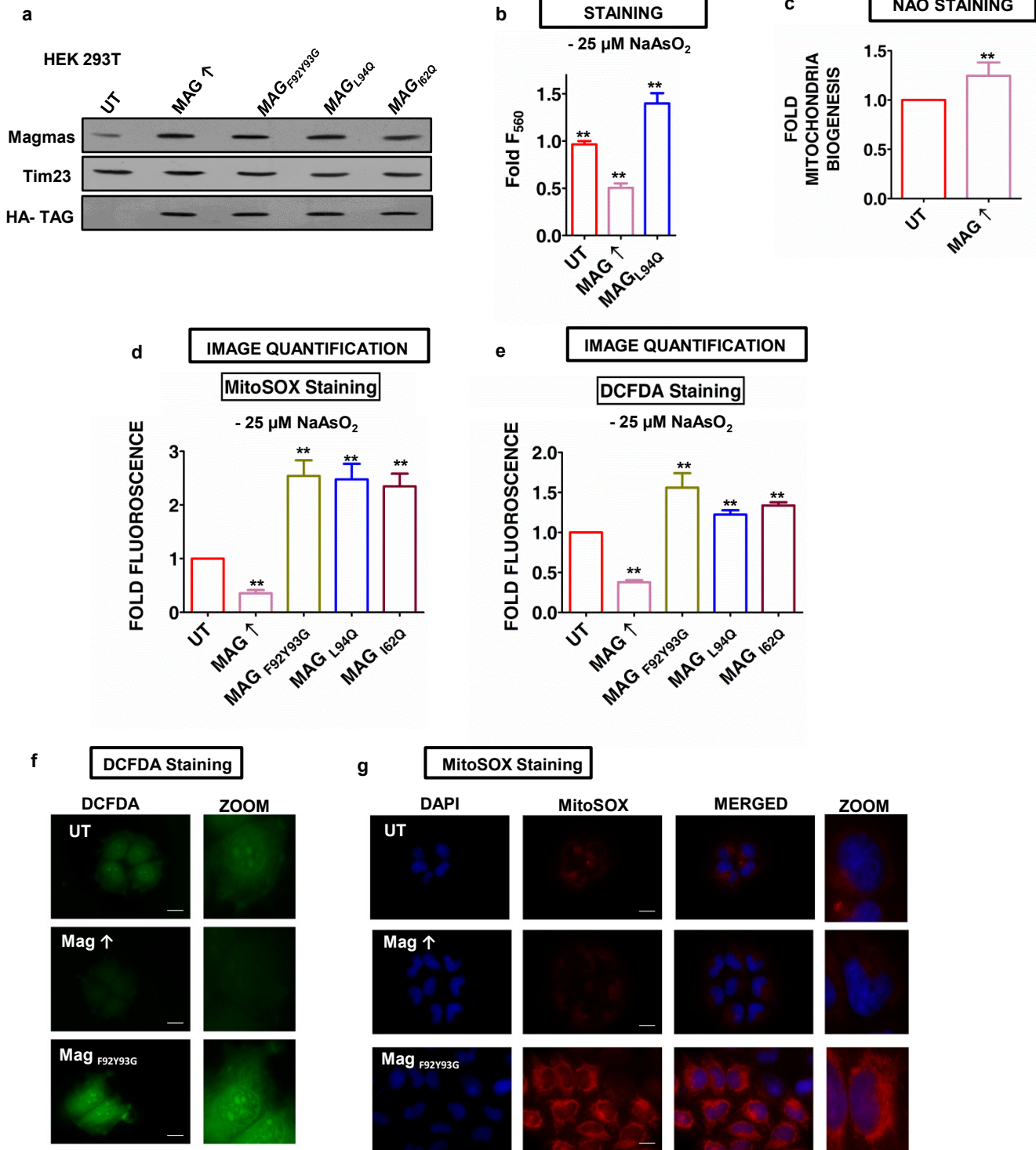


Figure S2 : (a) Western blot showing expression level of Magmas and Magmas mutants in HEK293T cells. (b) To measure the amount of cellular peroxides, HEK293T cells overexpressing Magmas were stained with Amplex red and peroxide level was represented as fold change in fluorescent intensity. (c) Flow cytometric analysis of mitochondria biogenesis using Nonyl Acridine Orange (NAO) staining in HEK293T cells overexpressing Magmas. (d, e) Quantification of change in fluorescent intensities of MitoSOX (d) and DCFDA (e) staining upon upregulation of Magmas and Magmas mutants in HeLa cells as observed by microscopic analysis (shown in Figure 2 f-e). Images were quantified by selecting equal area of respective fields corresponding to single cell, followed by quantification with the help of ImageJ. Data represented as mean \pm SEM, n=3, ***P* (two tailed). (f, g) Microscopic images of HeLa cells stained with DCFDA (f) and MitoSOX (g) using phenol red free medium.

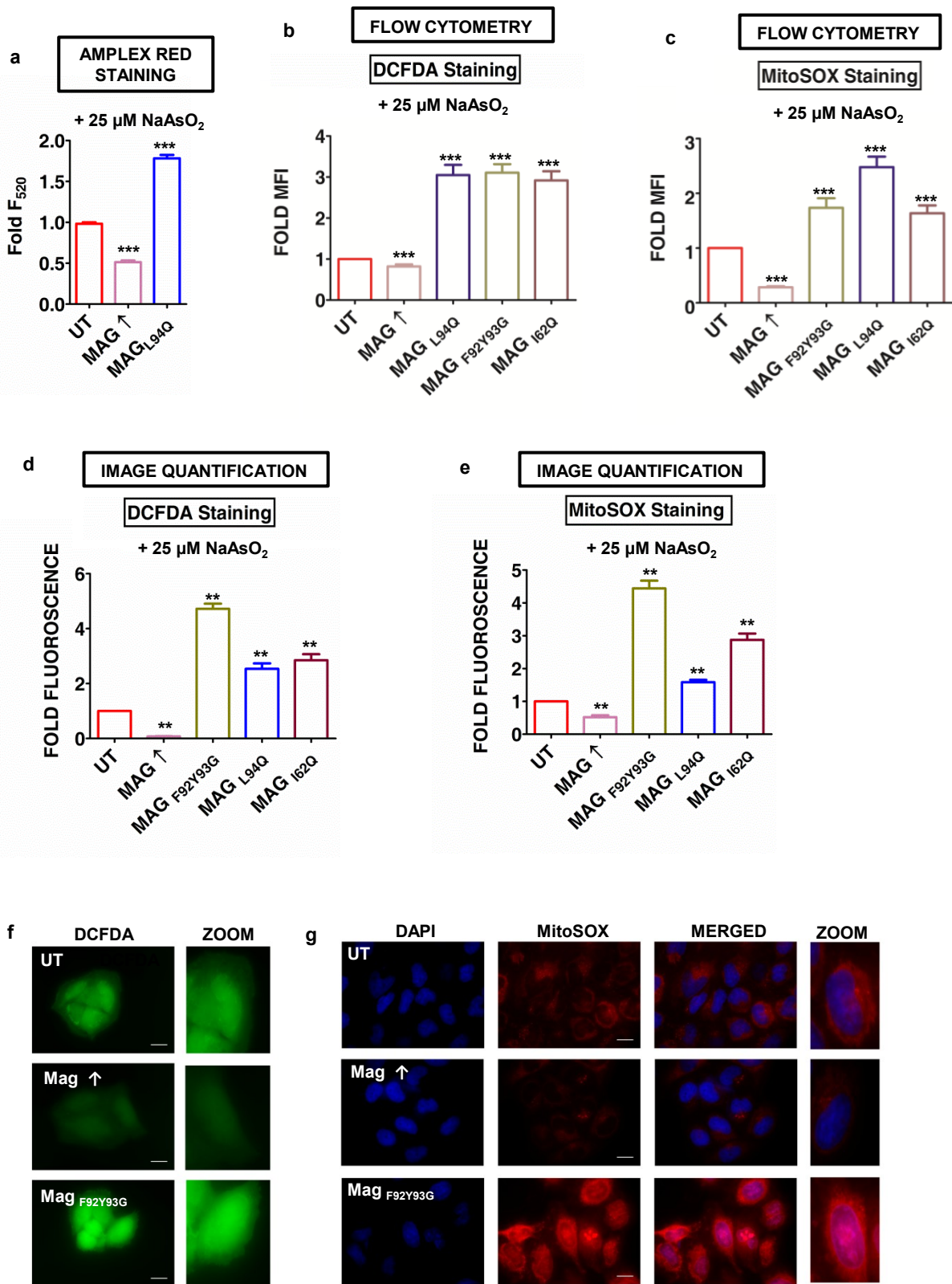


Figure S3 (a) Flow cytometric analysis of amplex red staining of cell overexpressing Magmas and treated with 25 μM NaAsO_2 . (b, c) Cellular ROS levels and mitochondrial superoxide levels in HEK293T cells expressing Magmas mutants were measured by DCFDA staining (b) and MitoSOX staining (c) respectively after treatment with 25 μM NaAsO_2 . (d, e) Quantification of images of HeLa cells overexpressing Magmas and its mutants (shown in Fig. 3 g-h) treated with 25 μM NaAsO_2 followed by staining with DCFDA (d) and MitoSOX (e) with the help of ImageJ. Change in fluorescent intensity was depicted as fold difference over untransfected HEK293T cells treated with 25 μM NaAsO_2 . Data represented as mean \pm SEM, $n=3$, $***P$ (two tailed) < 0.0001 , $**P$ (two tailed) < 0.001 . (f, g) Microscopic images of HeLa cells stained with DCFDA (f) and MitoSOX (g) using phenol red free medium.

Supplementary Figure S4

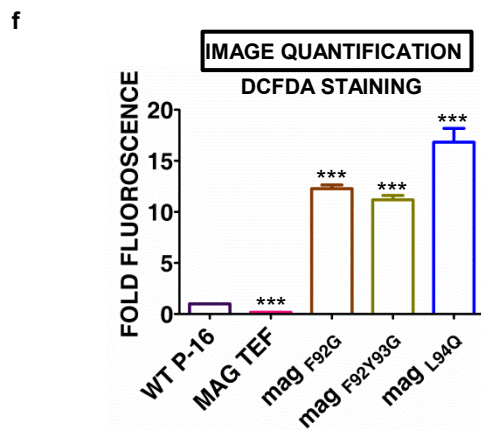
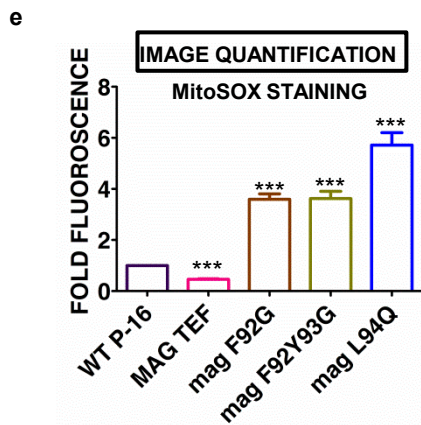
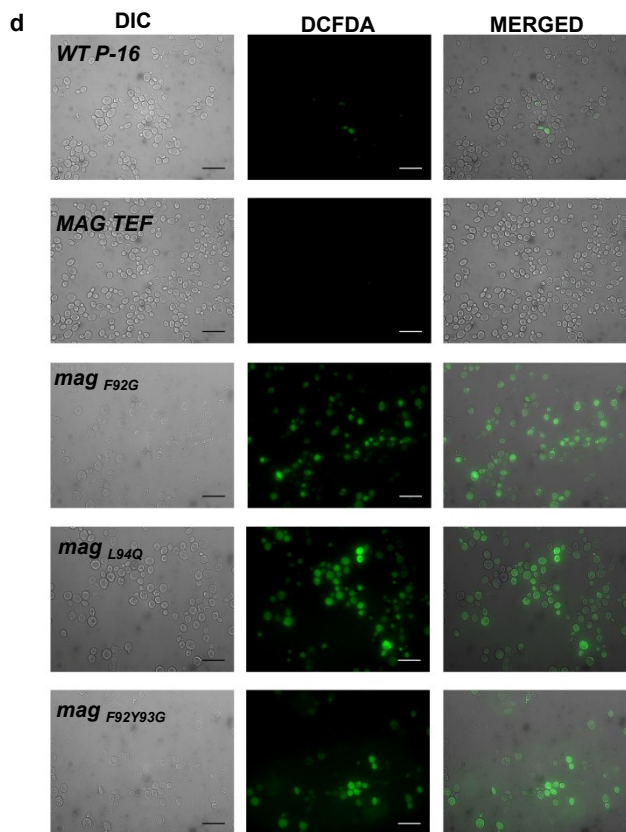
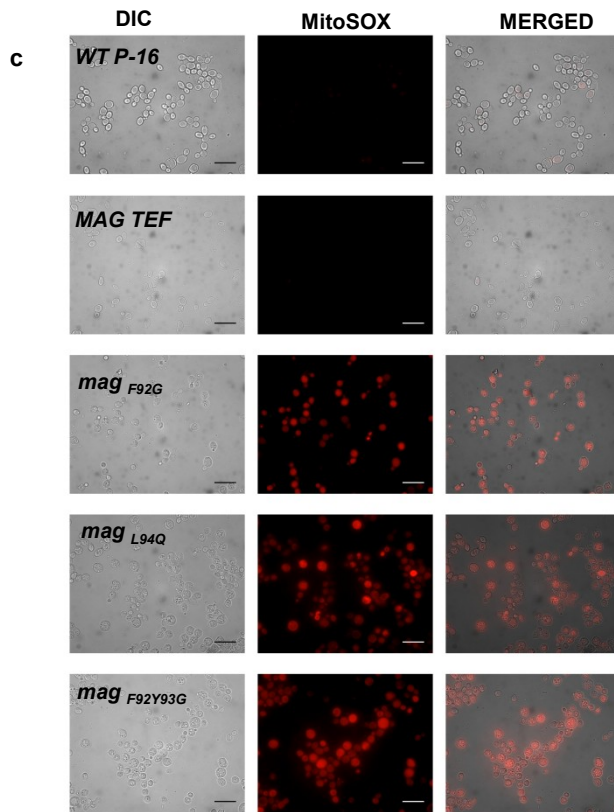
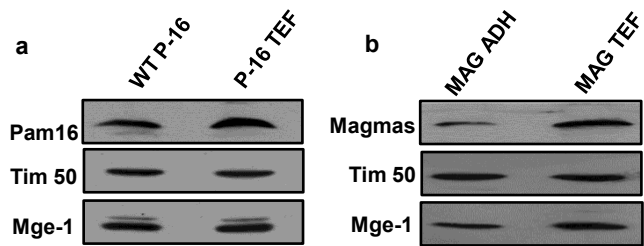


Figure S4 (a, b) Immunoblots showing the expression levels of Pam16 (a) and Magmas (b) in isolated mitochondria using anti-Pam16 and anti-Magmas antibody respectively. As a loading control anti-Tim50 and anti-Mge-1 antibody was used. (c, d) Microscopic images of mutant expressing yeast cells stained with MitoSOX (c) and DCFDA (d). Scale bar: 4 μm . (e, f) Quantification of microscopic images of yeast cells expressing Magmas and Magmas mutants stained with MitoSOX (e) and DCFDA (f) by ImageJ. Data represented as mean \pm SEM, $n=3$, *** P (two tailed) < 0.0001 .

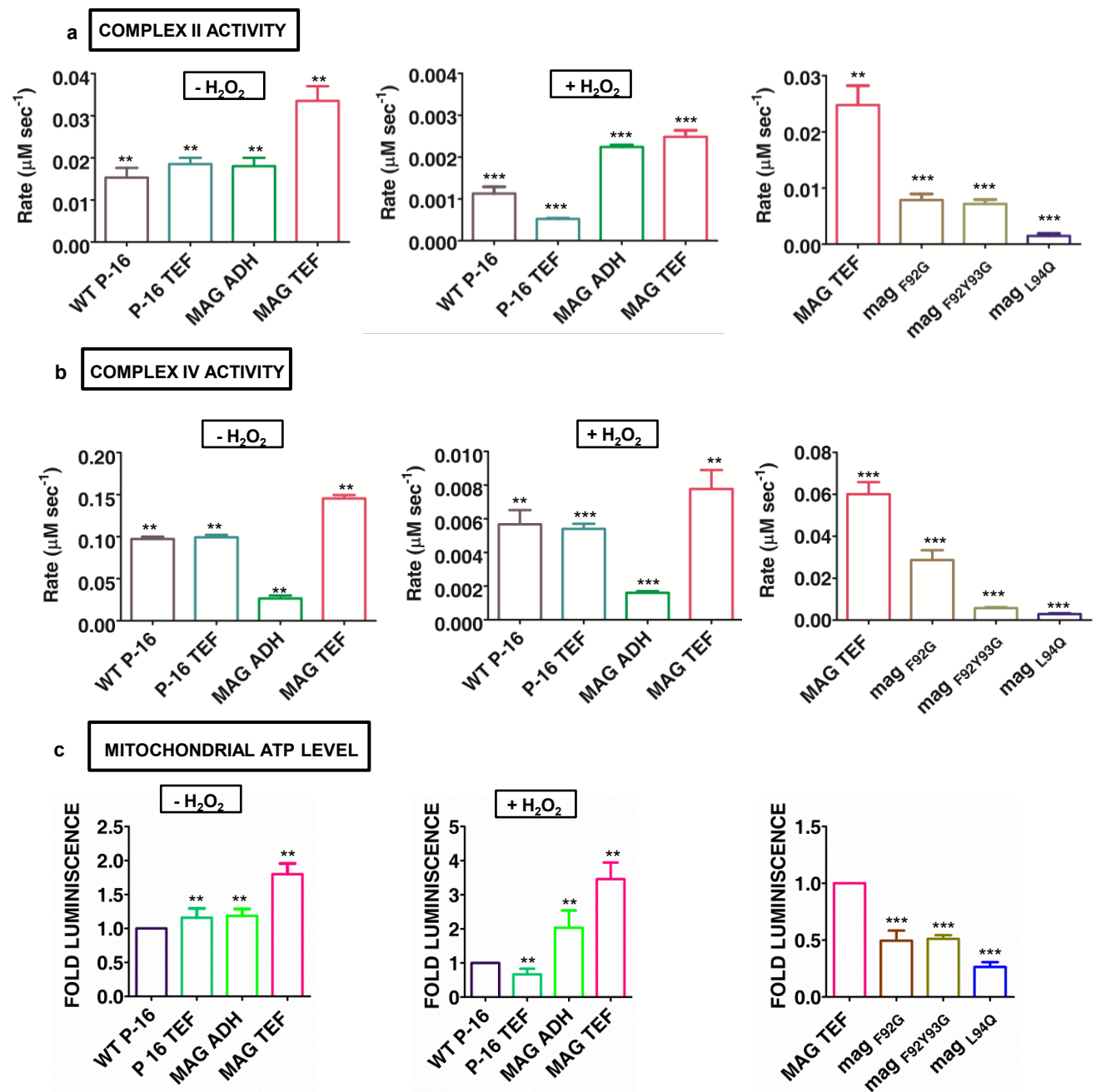


Figure S5 (a, b) Yeast cells expressing Magmas under *ADH* and *TEF* promoter were grown in a medium containing glycerol prior to isolation of mitochondria. To determine the effect of oxidative stress on ETC complex II and IV activity, cells were exposed to 4 mM H₂O₂ for 3 h 30 min at 30 °C before isolation of mitochondria. Isolated mitochondria were used for the assessment of ETC complex activity after permeabilization with 1% DOC as mentioned earlier. Effect of Magmas mutants on ETC complex activity was analyzed in absence of an external oxidative stress. (c) Mitochondrial ATP level was analyzed by using isolated mitochondria from respective yeast strains through Promega TOXGlo detection kit. Data represented as mean ± SEM, n=3, ****P* (two tailed) < 0.0001, ***P* (two tailed) < 0.05.

Supplementary Figure S6

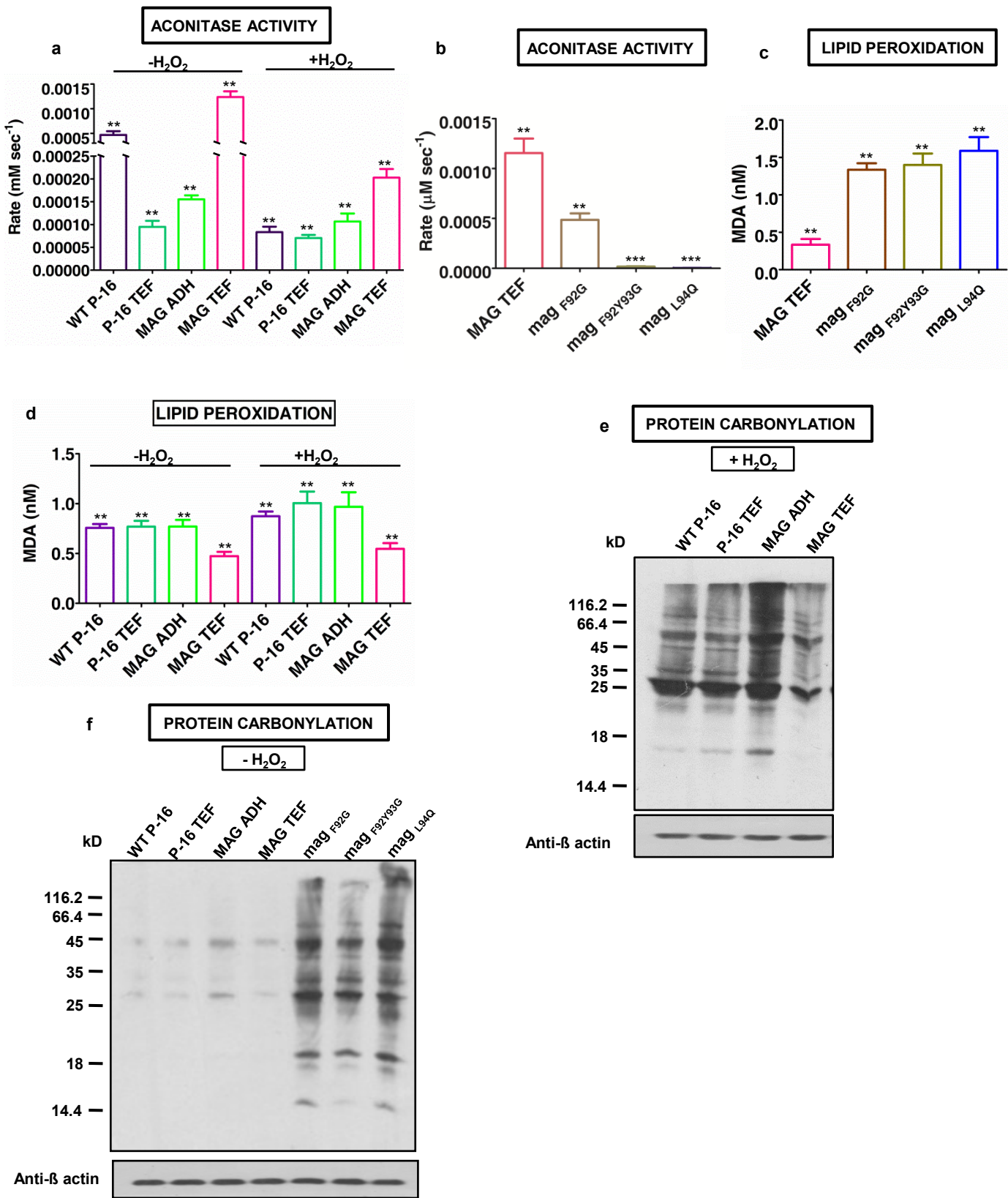


Figure S6 (a, b,) Aconitase activity measured in mitochondria isolated from yeast cells expressing different levels of Magmas and Pam16 in absence and presence of 4 mM H₂O₂ (a) and in mitochondria expressing Magmas mutants (b). (c, d) The damage to lipid in form of the peroxidation was detected through TBARS assay in yeast cells expressing Magmas mutants (c) and in cells expressing Magmas and Pam16, after an oxidative stress through 4 mM H₂O₂ (d). (e, f) The oxidative damage to protein through the carbonylation of protein side chains was detected by MilliPore OxyBlot™ Protein oxidation Detection Kit in cells expressing Pam16. Magmas and Magmas mutants (f) and cells expressing Pam16 and Magmas after an exposure to oxidative insult (e). Anti-β actin antibody was used a loading control. Data represented as mean ± SEM, n=3, ***P* (two tailed) <0.01, ****P* (two tailed) <0.001.

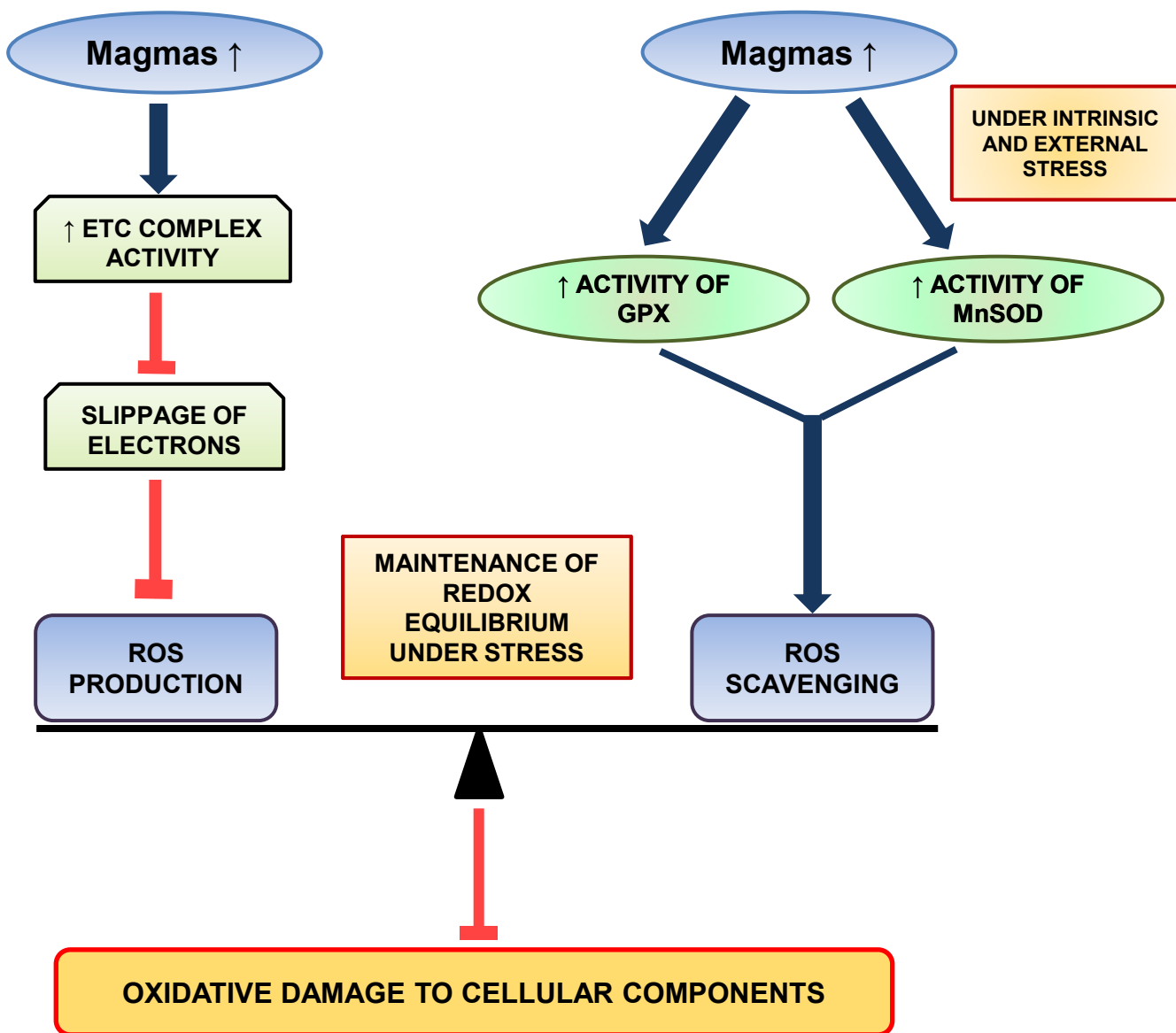


Figure S7. A schematic diagram showing the probable mechanism followed by Magmas to maintain the redox equilibrium. Magmas enhances the ETC complex activity leading to proper channeling of electrons, thereby reduces ROS production. Under external or internal stress, Magmas also promotes ROS scavenging by increasing the antioxidant activity of GPx and MnSOD. Thus, Magmas maintains ROS balance both at production as well as at scavenging level and prevents oxidative-stress mediated damage to cellular components.